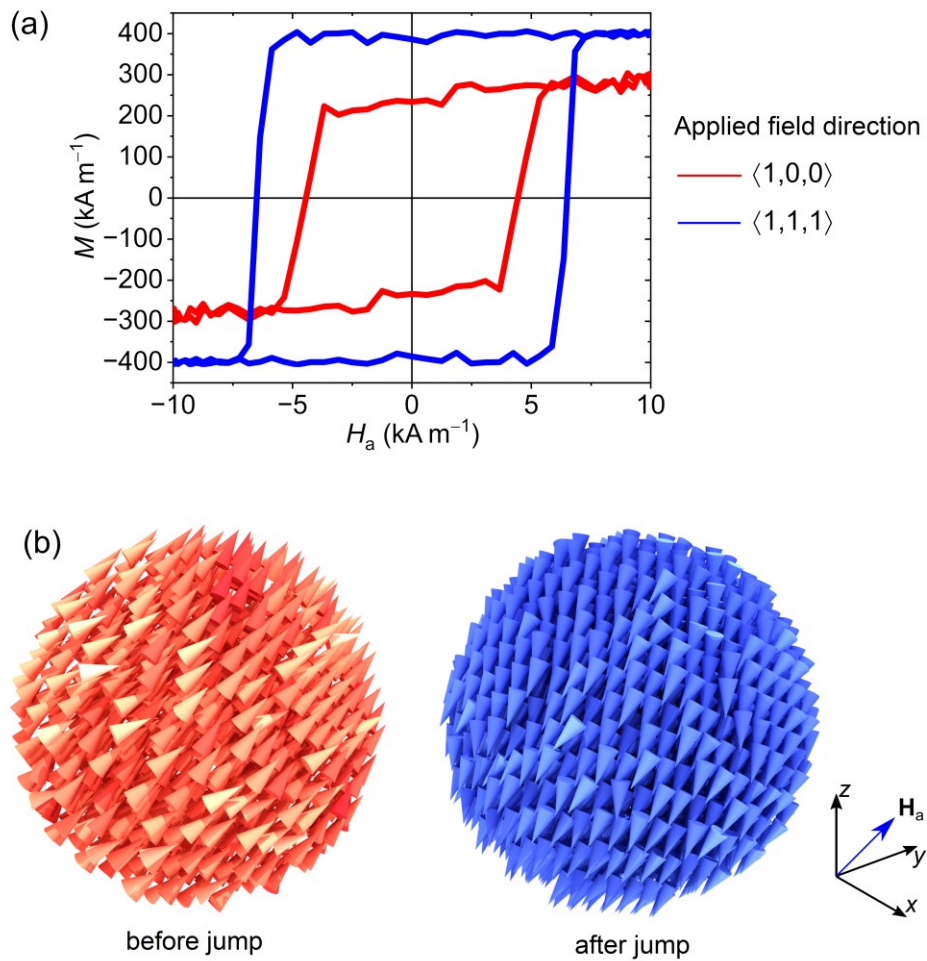


## **Electronic Supplementary Information**

### **Influence of size, aggregation state and excitation conditions on hyperthermia properties of magnetite nanoparticles**

Riccardo Ferrero,<sup>a</sup> Marta Vicentini<sup>a</sup> and Alessandra Manzin<sup>a</sup>

<sup>a</sup>Istituto Nazionale di Ricerca Metrologica (INRiM), Strada delle Cacce 91, 10135 Torino, Italy



**Fig. S1** 3D micromagnetic simulation of a  $\text{Fe}_3\text{O}_4$  nanosphere with 40 nm diameter, discretized with cubic cells of 2.5 nm size and having magnetocrystalline hard axes set along the Cartesian ones. (a) Comparison of the dynamic hysteresis loops calculated by applying a 100 kHz magnetic field with peak amplitude of  $10 \text{ kA m}^{-1}$  along the hard direction  $\langle 1,0,0 \rangle$  and easy direction  $\langle 1,1,1 \rangle$ . (b) Magnetization configurations at the time instants immediately before (left) and after (right) the irreversible jump along the descending branch of the hysteresis loop, calculated for the applied field direction  $\langle 1,1,1 \rangle$ .

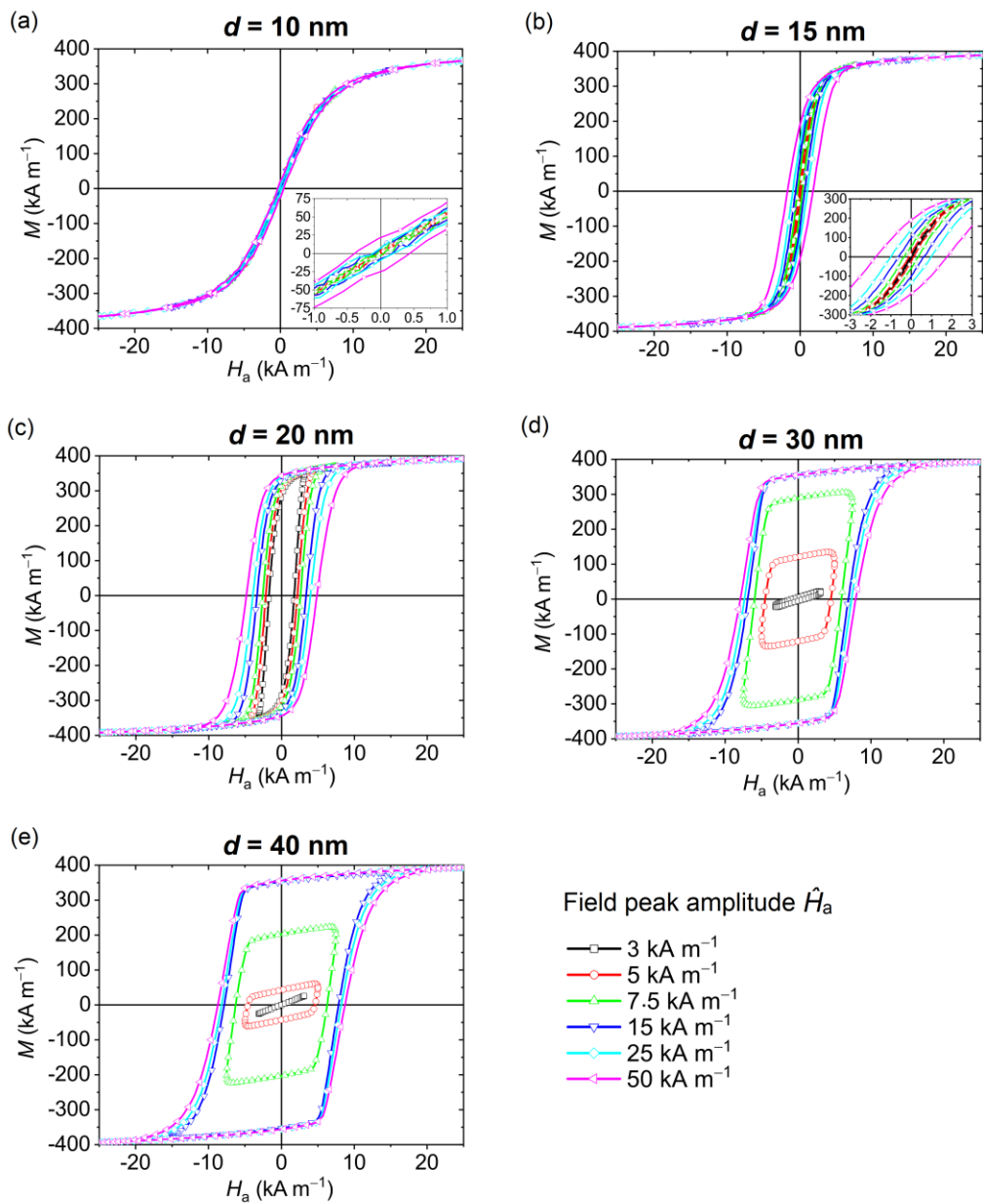


**Fig. S2** Dynamic hysteresis loops calculated for five samples of non-interacting Fe<sub>3</sub>O<sub>4</sub> NPs with size  $d$  fixed to (a) 10 nm, (b) 15 nm, (c) 20 nm, (d) 30 nm and (e) 40 nm. The frequency of the applied magnetic field is set at 200 kHz for all the simulations, and the peak amplitude  $\hat{H}_a$  varies between 3 and 50  $\text{kA m}^{-1}$ . Hergt-Dutz limit is fulfilled up to  $\hat{H}_a = 25 \text{ kA m}^{-1}$ .

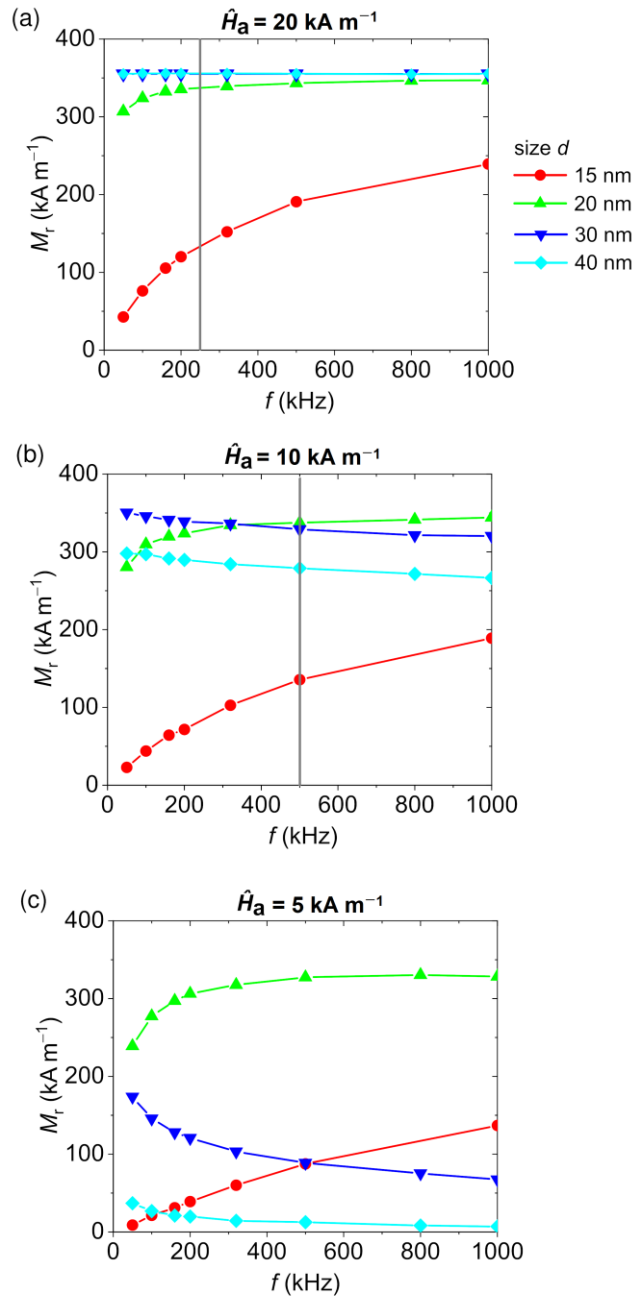


**Fig. S3** Influence of AC magnetic field frequency  $f$  on the remanent magnetization of four samples of non-interacting  $\text{Fe}_3\text{O}_4$  NPs with size  $d$  variable from 15 to 40 nm, fixing magnetic field peak amplitude  $\hat{H}_a$  to (a)  $20 \text{ kA m}^{-1}$ , (b)  $\hat{H}_a = 10 \text{ kA m}^{-1}$  and (c)  $\hat{H}_a = 5 \text{ kA m}^{-1}$ . In graphs (a) and (b) the vertical grey lines represent the Hergt-Dutz limit.

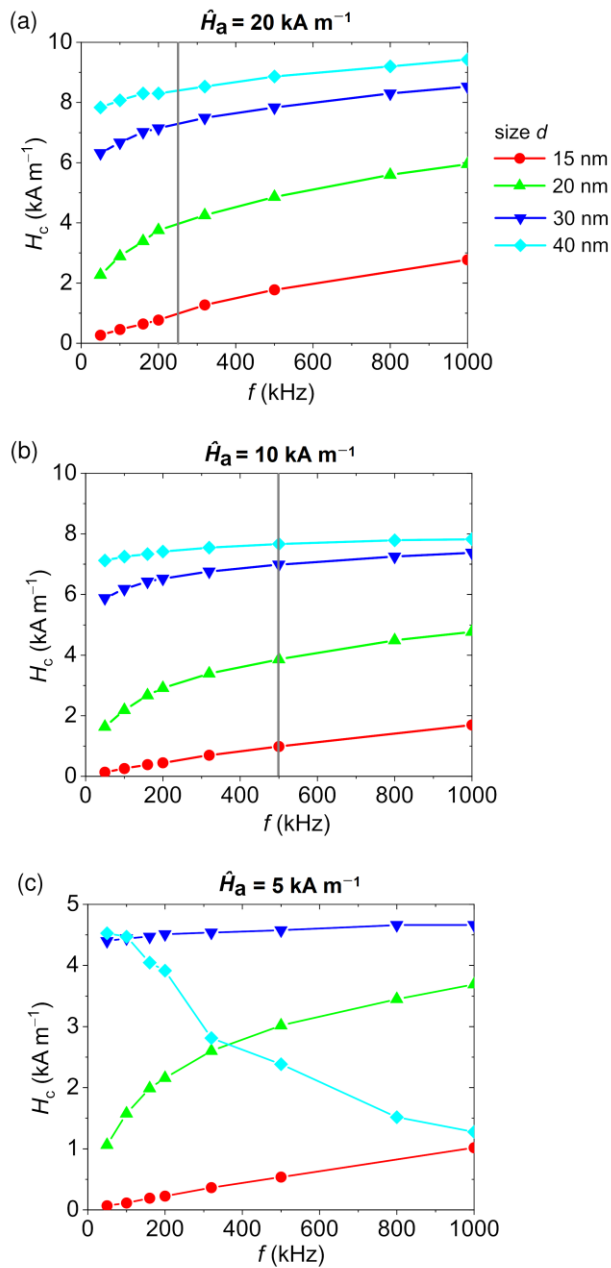


**Fig. S4** Influence of AC magnetic field frequency  $f$  on the coercivity of four samples of non-interacting  $\text{Fe}_3\text{O}_4$  NPs with size  $d$  variable from 15 to 40 nm, fixing magnetic field peak amplitude  $\hat{H}_a$  to (a)  $20 \text{ kA m}^{-1}$ , (b)  $\hat{H}_a = 10 \text{ kA m}^{-1}$  and (c)  $\hat{H}_a = 5 \text{ kA m}^{-1}$ . In graphs (a) and (b) the vertical grey lines represent the Hergt-Dutz limit.

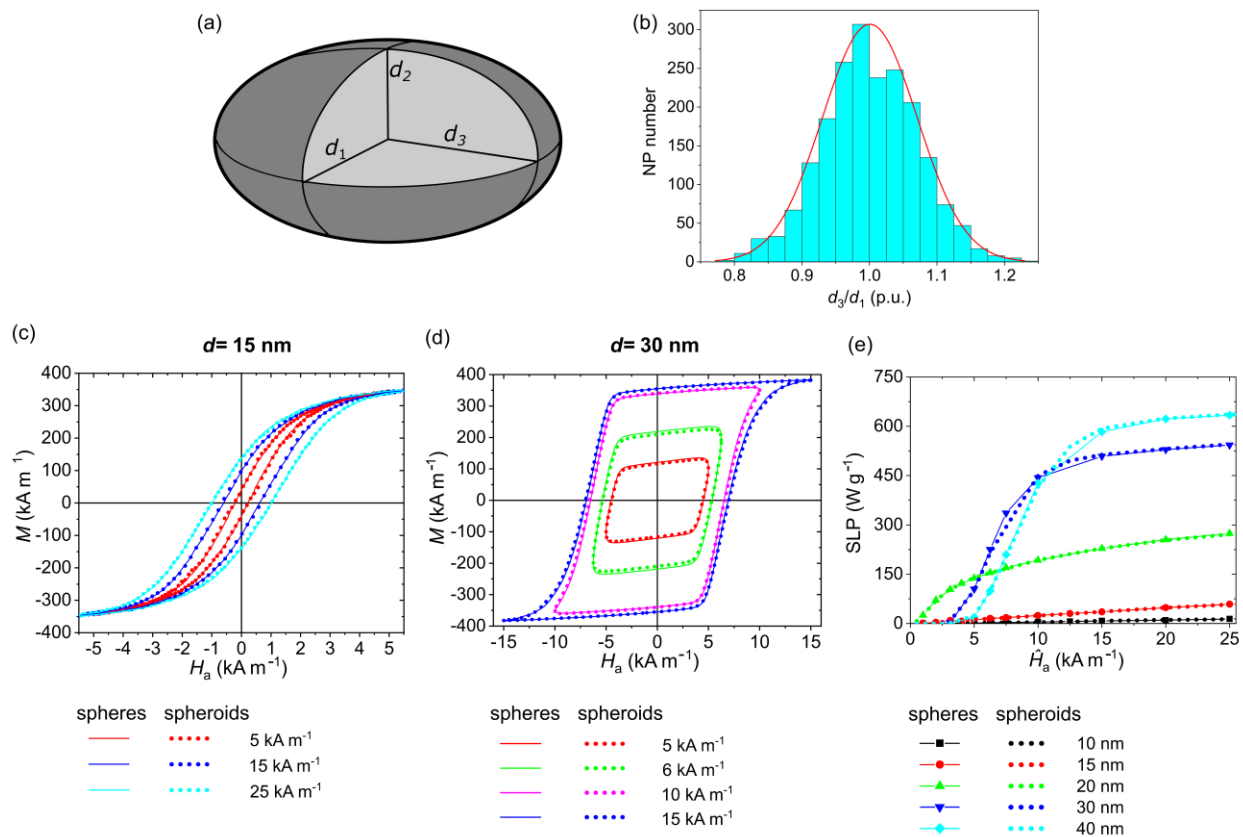


**Fig. S5** Results for ensembles of 2000 infinitely diluted  $\text{Fe}_3\text{O}_4$  NPs with randomly variable spheroidal shape around the spherical one. (a) Schematic of a spheroid, with aspect ratio  $d_3/d_1$ , where  $d_3$  is the length along the spheroid symmetry axis and  $d_1 = d_2$  is the equatorial diameter. (b) Considered Gaussian distribution of NP aspect ratios, with mean equal to 1 ( $d_1 = d_2 = d_3 = d$ ), standard deviation equal to 0.07, and NP volume fixed to  $\pi d^3/6$ . Dynamic hysteresis loops calculated at 200 kHz for variable magnetic field peak amplitude, setting  $d$  at (c) 15 nm and (d) 30 nm: comparison between random distributions (dotted lines) and ensembles with perfectly spherical NPs (continuous lines). (e) Specific loss power (SLP) calculated for  $d$  ranging from 10 to 40 nm: comparison between random distributions (dotted lines) and ensembles with perfectly spherical NPs (lines with markers).

### Regular grid distributions, $d = 15$ nm

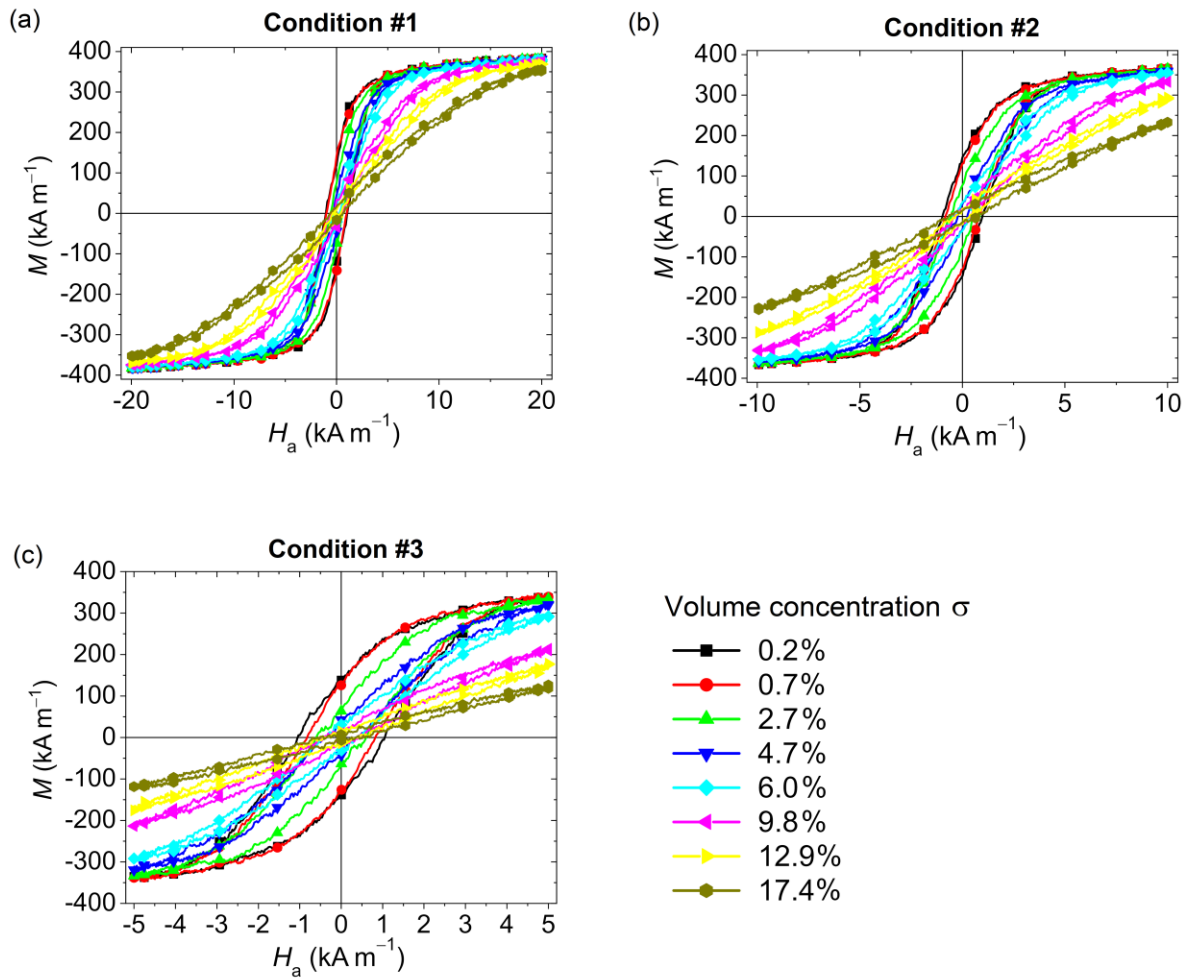


**Fig. S6** Dynamic hysteresis loops versus volume concentration  $\sigma$  for interacting 15 nm sized  $\text{Fe}_3\text{O}_4$  NPs distributed on 3D regular grids, calculated under three excitation conditions: #1 –  $\hat{H}_a = 20 \text{ kA m}^{-1}$ ,  $f = 250 \text{ kHz}$ ; #2 –  $\hat{H}_a = 10 \text{ kA m}^{-1}$ ,  $f = 500 \text{ kHz}$ ; #3 –  $\hat{H}_a = 5 \text{ kA m}^{-1}$ ,  $f = 1 \text{ MHz}$ .

Random distributions,  $d = 15$  nm

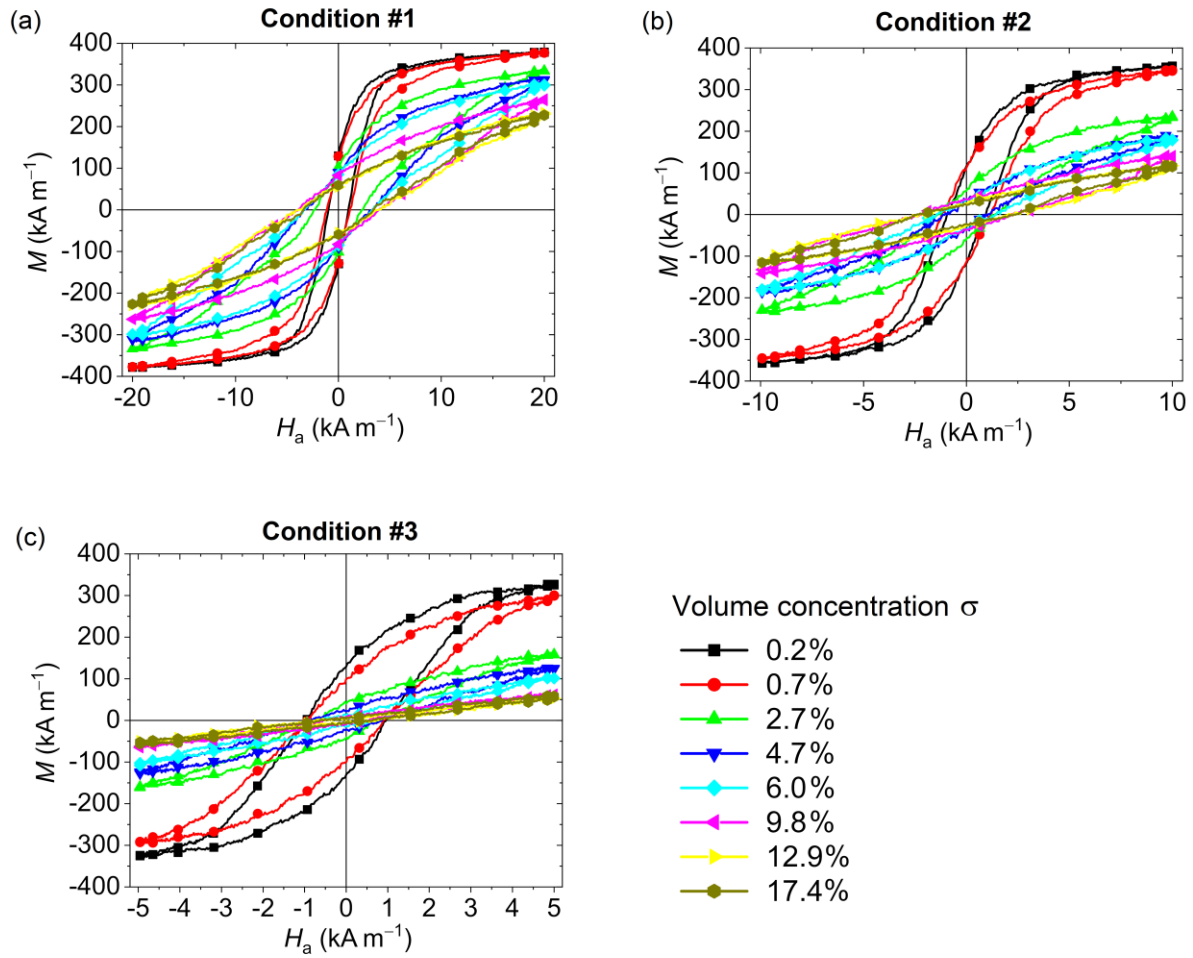


**Fig. S7** Dynamic hysteresis loops versus volume concentration  $\sigma$  for interacting 15 nm sized  $\text{Fe}_3\text{O}_4$  NPs randomly distributed in the space, calculated under three excitation conditions: #1 –  $\hat{H}_a = 20 \text{ kA m}^{-1}$ ,  $f = 250 \text{ kHz}$ ; #2 –  $\hat{H}_a = 10 \text{ kA m}^{-1}$ ,  $f = 500 \text{ kHz}$ ; #3 –  $\hat{H}_a = 5 \text{ kA m}^{-1}$ ,  $f = 1 \text{ MHz}$ .



### Regular grid distributions, $d = 30$ nm

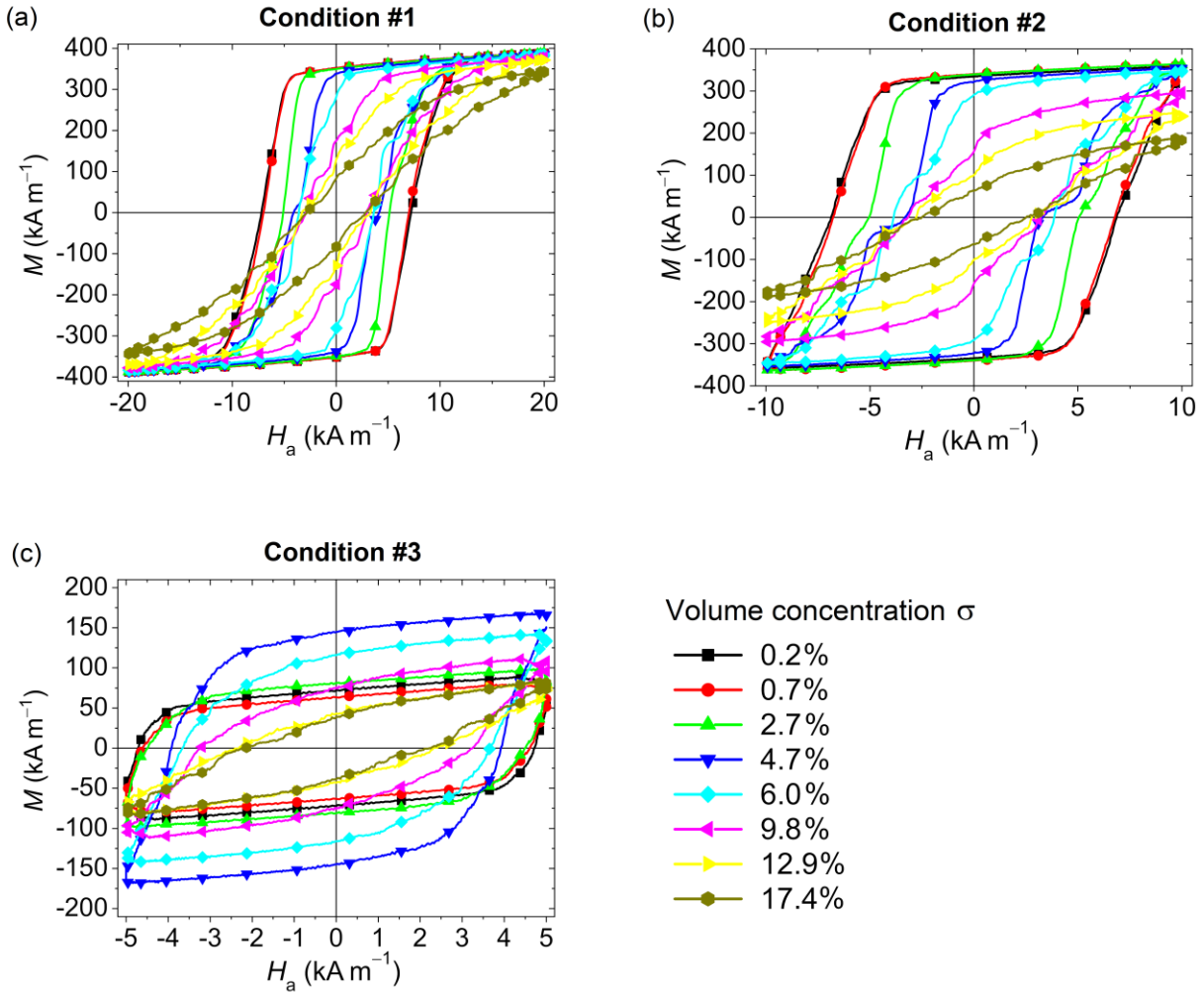


**Fig. S8** Dynamic hysteresis loops versus volume concentration  $\sigma$  for interacting 30 nm sized  $\text{Fe}_3\text{O}_4$  NPs distributed on 3D regular grids, calculated under three excitation conditions: #1 –  $\hat{H}_a = 20 \text{ kA m}^{-1}$ ,  $f = 250 \text{ kHz}$ ; #2 –  $\hat{H}_a = 10 \text{ kA m}^{-1}$ ,  $f = 500 \text{ kHz}$ ; #3 –  $\hat{H}_a = 5 \text{ kA m}^{-1}$ ,  $f = 1 \text{ MHz}$ .

### Random distributions, $d = 30$ nm

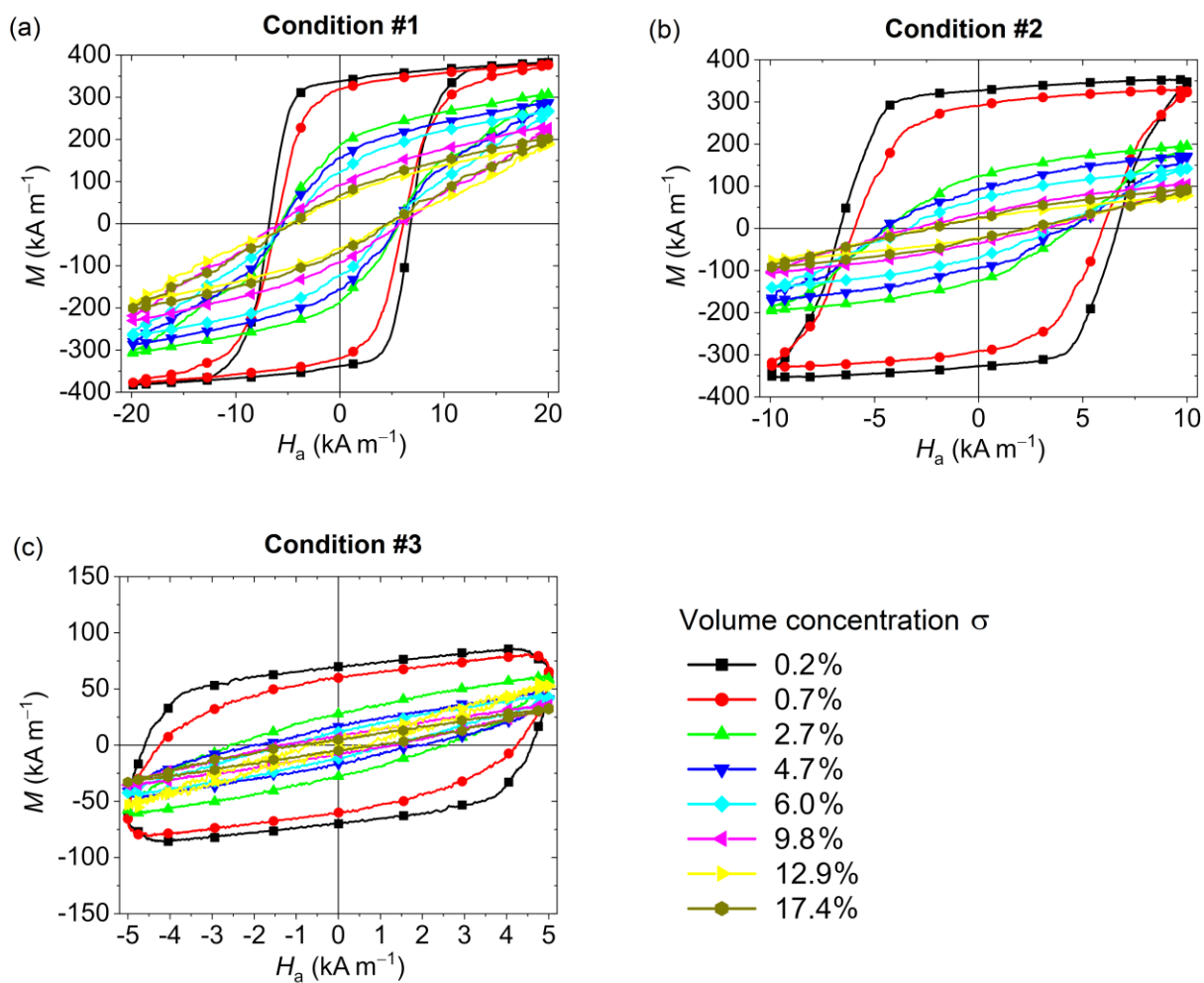


**Fig. S9** Dynamic hysteresis loops versus volume concentration  $\sigma$  for interacting 30 nm sized  $\text{Fe}_3\text{O}_4$  NPs randomly distributed in the space, calculated under three excitation conditions: #1 -  $\hat{H}_a = 20 \text{ kA m}^{-1}$ ,  $f = 250 \text{ kHz}$ ; #2 -  $\hat{H}_a = 10 \text{ kA m}^{-1}$ ,  $f = 500 \text{ kHz}$ ; #3 -  $\hat{H}_a = 5 \text{ kA m}^{-1}$ ,  $f = 1 \text{ MHz}$ .